Theoretical study on longitudinally pumped $Yb^{3+}:Y_2O_3$ lasers

Haixia Ma (马海霞), Qihong Lou (楼祺洪), Yunfeng Qi (漆云凤), Jingxing Dong (董景星), and Yunrong Wei (魏运荣)

Shanghai Institute of Optics and Fine Mechanics, Chinese Academy of Sciences, Shanghai 201800

Received July 21, 2004

To optimize the performance of longitudinally pumped $Yb^{3+}:Y_2O_3$ ceramic lasers, cavity parameters such as material length and output coupler transmission at a certain laser output power are calculated numerically using quasi-three-level laser model. The results show great potential of $Yb^{3+}:Y_2O_3$ ceramics for highly efficient diode-pumped solid-state lasers.

OCIS codes: 140.3480, 140.3580, 140.5680.

Yb^{3+}-doped laser materials are very attractive for ultrashort pulse lasers as well as high-power solid-state lasers due to their broad absorption and emission bandwidths. Y_2O_3 is a promising solid-state laser material for trivalent lanthanide activators because of its some favorable properties, such as refractory nature, stability, and optical clarity over a broad spectral region. Thermal conductivity of Y_2O_3 is much larger than that of YAG, and their thermal expansion coefficients are very similar[1]. However, it is not feasible to obtain large size Y_2O_3 single crystals with sufficient optical quality by conventional melt-growth methods due to its melting temperature of 2430 °C and structure phase transition at 2280 °C. Therefore, there have been few reports on the Yb^{3+} doped Y_2O_3 lasers[2].

Recently, highly transparent ceramics have been fabricated using the liquid-phase chemical reaction and non-press vacuum sintering method[3,4]. The quality and the size of the ceramics have been improved greatly and highly efficient laser oscillations have been obtained[1,2,5]. However, the performance of the $Yb^{3+}:Y_2O_3$ ceramic lasers has not been optimized. In this paper, we calculate numerically cavity parameters to optimize the performance of $Yb^{3+}:Y_2O_3$ ceramic lasers.

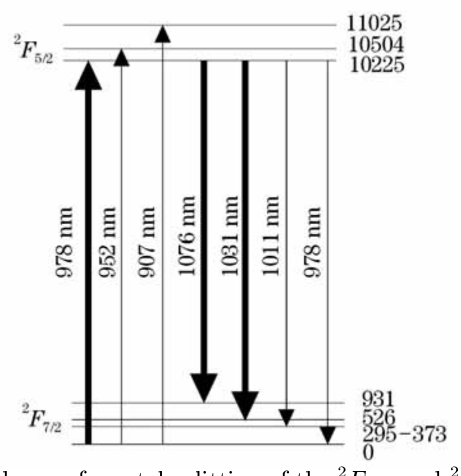

Fig. 1. Scheme of crystal splitting of the $^2F_{7/2}$ and $^2F_{5/2}$ levels of Yb^{3+} ions in Y_2O_3 laser. The levels of the upper and lower manifolds and their energies are shown. The laser transition is noted by the heavy line. The populations of the upper and lower laser levels are given by N_2 and N_1, respectively.

Yb^{3+}-doped Y_2O_3 laser is a typical quasi-three-level system. The energy level diagram of Yb^{3+} ions is shown in Fig. 1[6]. The Yb^{3+} ions have two $4f^{13}$ manifolds, $^2F_{5/2}$, and $^2F_{7/2}$, with energy gap of about 10225 cm^{-1}. The upper laser level is the lowest of the three crystal-field components of $^2F_{5/2}$ state. To the laser transition at 1076 nm, the lower laser level is the uppermost of the four crystal-field components of $^2F_{7/2}$ state. To the laser transition at 1031 nm, the lower laser level is the third crystal-field component of $^2F_{7/2}$ state. Assuming that relative populations of the levels can be described by a Boltzman distribution, the actual population densities in the lower and upper laser levels can be written as[7]

$$N_1 = \frac{g_1 N_L}{Z_L}\exp(-E_1/kT) = f_1 N_L, \quad (1)$$

$$N_2 = \frac{g_2 N_U}{Z_U}\exp(-E_2/kT) = f_2 N_U, \quad (2)$$

where Z_L and Z_U are the partition functions of the lower and upper states, respectively, which are defined as

$$Z_L = \sum_i g_i \exp(-E_i/kT),$$

$$Z_U = \sum_j g_j \exp(-E_j/kT), \quad (3)$$

where g_i and g_j are the degeneracies of the lower and upper states, respectively. For the Yb^{3+} ions in Y_2O_3 laser material, $g_i = g_j$=1. E_i and E_j are measured from the lowest crystal-field component of $^2F_{7/2}$ and $^2F_{5/2}$ states, respectively, N_L and N_U are the total population densities of the $^2F_{7/2}$ and $^2F_{5/2}$ states, and f_1 and f_2 are the fractional populations in the lower and upper laser levels, respectively.

The formula of laser threshold has been obtained from the rate equations describing the population inversion and the photon density in the laser cavity in the steady-state case[8]

$$P_{th3} = \frac{\pi h\gamma_p \left(w_l^2 + w_p^2\right)\left(L + T + 2N_1^0\sigma_{em} l\right)}{4\sigma_{em}\tau\eta_p\eta_a\left(f_1 + f_2\right)}, \quad (4)$$

Table 1. Spectroscopic Parameters of the 10 at.-% Yb^{3+}:Y_2O_3 Ceramics

Material	λ_p (nm)	σ_p ($\times10^{-20}$ cm^2)	τ (ms)	λ_{em} (nm)	σ_{em} ($\times10^{-20}$ cm^2)	f_1	f_2	N_1^0 ($\times10^{20}$ cm^{-3})
Transparent Ceramic	976	2.4[10]	0.82[4]	1031	0.92[10]	0.06	0.78	1.25
				1076	0.36[10]	0.009		0.18

where $h\gamma_p$ is the pump photon energy, w_l is the laser-beam waist, w_p is the pump-beam waist, L is intrinsic cavity loss, T is the output coupler (OC) transmission, N_1^0 is the unpumped population-inversion density of the lower laser level, σ_{em} is the gain cross section, τ is the lifetime of the upper manifold, $\eta_a = 1 - \exp(-\alpha l)$ is the fraction of incident pump power absorbed in a crystal of length l with absorption coefficient α, η_p is the pump quantum efficiency. The pumping process is assumed to have unity quantum efficiency.

Let $w_l = w_p$, the laser output power can be obtained from[7]

$$1 + \frac{B}{fS}\ln(1+fS) = fF\left[\frac{1}{fS} - \frac{1}{(fS)^2}\ln(1+fS)\right], \quad (5)$$

where $f = f_1 + f_2$, $B = \frac{2N_1^0\sigma_{em}l}{L+T}$, $F = \frac{4P_p\tau\sigma_{em}\eta_a\eta_p}{\pi h\gamma_p w_l^2(L+T)}$, $S = \frac{2c\sigma_{em}\tau\Phi}{n\pi w_l^2 l}$, c is the velocity of light in vacuum, n is the refractive index, P_p is the incident pump power, the total number Φ of laser photons in the cavity is given by $\Phi = \frac{2nlP_L}{ch\gamma_L}$, where P_L is the laser power traveling in one direction inside the cavity and γ_L is the laser frequency, the laser output power $P_{out} = P_L T$.

The optical properties of ceramics are very similar with those of single crystals[9], so we can optimize the performance of ceramic lasers by the optical properties of single crystals. The spectroscopic parameters of 10 at.-% Yb^{3+}-doped Y_2O_3 are listed in Table 1. There exists the strongest absorption peak centered at 976 nm in the absorption spectrum of the Yb^{3+}:Y_2O_3 ceramics, so a diode laser at 976-nm wavelength is used to longitudinally pump Yb^{3+}:Y_2O_3 ceramics.

At the laser output power of 6 W, the incident pump power of the laser at 1031-nm wavelength versus OC transmission and material length is plotted according to Eq. (5) in Fig. 2. In calculation, we use the parameters $w_p = w_l = 150$ μm and $L = 0.6\%$. Figure 2 shows that OC transmission and material length have a great influence on incident pump power. When the OC transmission is a constant, there exists a length which minimizes the incident pump power; when the material length is a constant, there exists an OC transmission which minimizes the incident pump power too. In the conditions considered, the incident pump power is at its minimum of 11.64 W when the material length is 0.5 mm and the OC transmission is 6%. The corresponding lasing threshold power is 2.25 W, the slope efficiency is 66%, and the optical-optical conversion efficiency is 51.5%. When the laser output power increases, the optimum material length and the OC transmission increase too. For example, at the laser output power of 1 W, the optimum material length is 0.35 mm and OC transmission is 3%; at the laser output power of 10 W, the optimum material length is 0.6 mm and OC transmission is 8%.

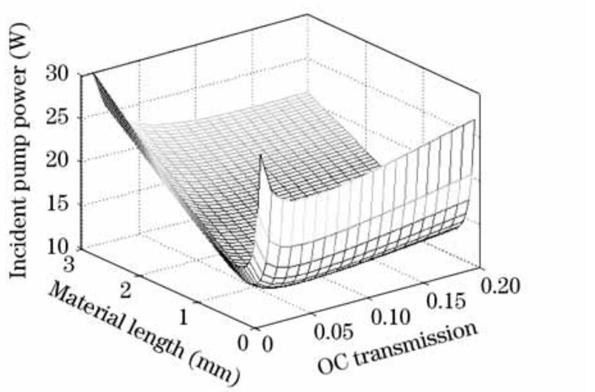

Fig. 2. Incident pump power of the laser at 1031-nm wavelength versus OC transmission and material length at the laser output power of 6 W.

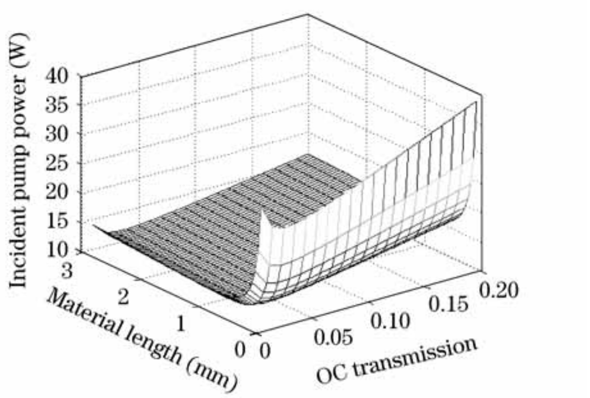

Fig. 3. Incident pump power of the laser at 1076-nm wavelength versus OC transmission and material length at the laser output power of 6 W.

Similarly, Fig. 3 shows the incident pump power of the laser at 1076-nm wavelength as a function of OC transmission and material length at the laser output power of 6 W. When the material length is 0.9 mm and the OC transmission is 3%, the performance of the laser at 1076-nm wavelength is optimized with the lasing threshold power of 1.49 W, the incident pump power of 10.55 W, the corresponding slope efficiency of 67%, and the optical-optical conversion efficiency of 56.9%.

We have presented an analysis of the performance of longitudinally pumped quasi-three-level Yb^{3+}:Y_2O_3 lasers. At the laser output power of 6 W, the laser at 1031-nm wavelength can be optimized with the slope efficiency of 66%, the optical-optical conversion efficiency of 51.5% at the material length of 0.5 mm and the OC transmission of 6%. The laser at 1076-nm wavelength can be optimized with the slope efficiency of 67% and optical-optical conversion efficiency of 56.9% at the material length of 0.9 mm and the OC transmission of 3%. The performance of Yb^{3+}:Y_2O_3 lasers is optimized by choosing an appropriate material length and an appropriate OC transmission at a certain laser output power. The calculated results show great potential of Yb^{3+}:Y_2O_3 ceramics for highly efficient diode-pumped solid-state lasers.

H. Ma's e-mail address is mahaixia1976@sina.com.

References

1. K. Takaichi, H. Yagi, J. Lu, J. F. Bisson, A. Shirakawa, K. Ueda, T. Yanagitani, and A. A. Kaminskii, Appl. Phys. Lett. **84,** 317 (2004).
2. J. Lu, K. Takaichi, T. Uematsu, A. Shirakawa, M. Musha, K. Ueda, H. Yagi, T. Yanagitani, and A. A. Kaminskii, Jpn. J. Appl. Phys. **41,** L1373 (2002).
3. T. Yanagitani, H. Yagi, and M. Ichikawa, Japanese Patent 10-101333 (1998).
4. T. Yanagitani, H. Yagi, and Y. Hiro, Japanese Patent 10-101411 (1998).
5. J. Kong, D. Y. Tang, J. Lu, K. Ueda, H. Yagi, and T. Yanagitani, Opt. Lett. **29,** 1212 (2004).
6. L. Laversenne, Y. Guyot, C. Goutaudier, M. Th. Cohen-Adad, and G. Boulon, Opt. Mater. **16,** 475 (2001).
7. C. Li, Y. J. Huo, S. F. He, and Y. H. Cao, Acta Opt. Sin. (in Chinese) **18,** 1473 (1998).
8. W. P. Risk, J. Opt. Soc. Am. B **5,** 1412 (1988).
9. J. Lu, M. Prabhu, K. Ueda, H. Yagi, T. Yanagitani, A. Kudryashov, and A. A. Kaminskii, Laser Phys. **11,** 1053 (2001).
10. K. Petermann, G. Huber, L. Fornasiero, S. Kuch, E. Mix, V. Peters, and S. A. Basun, J. Lumin. **87,** 973 (2000).